SAE INTERNATIONAL

Combining Thermodynamics and Design Optimization for Finding ICE Downsizing Limits

2014-01-1098
Published 04/01/2014

Sergii Bogomolov, Vit Dolecek, Jan Macek, Antonin Mikulec, and Oldrich Vitek
Czech Technical University

CITATION: Bogomolov, S., Dolecek, V., Macek, J., Mikulec, A. et al., "Combining Thermodynamics and Design Optimization for Finding ICE Downsizing Limits," SAE Technical Paper 2014-01-1098, 2014, doi:10.4271/2014-01-1098.

Abstract

The mass and overall dimensions of massively downsized engines for very high bmep (up to 35 bar) cannot be estimated by scaling of designs already available. Simulation methods coupling different levels of method profoundness, as 1-D methods, e.g., GT Suite/GT Power with in-house codes for engine mechanical efficiency assessment and preliminary design of boosting devices (a virtual compressor and a turbine), were used together with optimization codes based on genetic algorithms. Simultaneously, the impact of optimum cycle on cranktrain components dimensions (especially cylinder bore spacing), mass and inertia force loads were estimated since the results were systematically stored and analyzed in Design Assistance System DASY, developed by the authors for purposes of early-stage conceptual design.

General thermodynamic cycles were defined by limiting parameters (bmep, burning duration, engine speed and turbocharger efficiency only). The unprejudiced assessment was based on variability of any other engine design feature. Holistic approach to all engine systems impacting brake efficiency and sensitivity analysis to yet unknown parameters occurred to be very robust tool with sometimes surprising results, giving impulse for the future engine research. The shortest combustion angle or unlimited peak pressure has not yielded the best results due to the same reasons. Too large stroke is disabled by mechanical efficiency, too small speed due to wall heat loss. Too efficient internal cycle leaves too small energy for a TC drive. Brake efficiency reached for passenger car engine is less than 50% if no waste heat regeneration is employed. The mass of cranktrain was estimated for limited fatigue safety factor and bearing loads.

Comprehensive approach to iterative concept and configuration/parametric optimizations of thermal machines with internal combustion explained the limits achievable in the future. The procedures were described and stored in DASY environment. Coupling of the results to lightweight vehicles with properly scaled individual components and accessories of downsized/downspeeded engines is possible in this approach. Although not all methods for reaching the predicted optimum parameters have been already mastered, the study presents good base for finding new engine layouts and assessing their feasibility already in the concept phase.

Introduction

Downsizing is often referred to as a way for increasing engine brake efficiency (due to reduction of relative thermal and mechanical losses) and improving road fuel consumption due to higher load of an engine in operation. Simultaneously, engine size and mass are reduced, which is accompanied by vehicle driving resistance decrease. On the other hand, much higher peak pressures occur, which has to be taken into account in dimensioning engine components. More robust components increase relatively the engine mass and cost. The peak pressures and inertia forces of heavier moving components impact mechanical losses in a cranktrain. In the case of any of apparently high-efficient low-temperature combustion systems (e.g., HCCI, PCCI or RCCI), efficient boost pressure charging of cylinders is required due to mixture dilution but often it is not taken into account during optimization.

Downsizing may be accompanied by downspeeding, reflected in lower cycle frequency (speed in rpm). Despite all efforts, the real limits of design have not yet been found - [1] and [2]. It is worthwhile mentioning the different level of optimism of industrial and academic R&D, in which the former is limited to very conservative level but the latter one tends to overestimate the results already achieved. Similar issues had been already addressed in the 50's of the last century by Eichelberg and Zinner (concluded by experiments with real medium speed, large bore, high air excess, crosshead four stroke test engine at MAN Augsburg), which was repeated by Syassen again for large bore four stroke engines in the 70's. Recently, the same issues of truck and passenger car engines were addressed -

e.g., [3] and [4]. The optimum solution depends on the total effects of new design on a new product. Moreover, the described issues should be optimized for real driving conditions, hopefully reflected in test procedures, considering both fuel efficiency together with CO2 and other GHG emissions fulfilling future pollution standards.

Up to now, no clear way to totally optimum downsized engine has been found during years of pressure charging application for ICEs. The main issue is in difficult early stage decision of a new engine design concept considering future (yet not designed) vehicle performance. The conservative approach of engine designers is based on necessity using experience and design heritage of every manufacturer, which has limited the constraints or any optimization for industrial purposes. Moreover, the immediate practical usage of results forces the researcher to find fast the compromised (geometrical) parameters, which cannot be easily changed in operation (up to now typically stroke or connecting rod length, in some cases even geometrical compression ratio).

The tools for doing this uneasy task and results of fully optimized downsized engine are being intensively developed, which is, e.g., described in the current paper as a continuation of authors' previous studies - [5] and [8]. This first attempt to optimize both efficiency and engine mass accompanied by main design parameters estimation at different loads/speeds will be followed by powertrain and vehicle design changes including powertrain control systems in the near future.

For this preliminary study, a really existing four cylinder, diesel engine of 1.65 dm^3 displacement volume has been used. Unlike in other published studies, the optimization of brake specific fuel consumption was done using minimal number of constraints to find the total optimum. The efficient exhaust gas aftertreatment system (like SCR) is assumed, which sets almost no limits to thermodynamic optimization. The low-temperature combustion modes are implicitly taken into account, as well, using two cases of rather short combustion duration combined with the mentioned high level of freedom during optimization.

The goal of this effort is to find the optimum envelope of possibilities limiting any future real solution. The partially optimized realizable designs with reduced flexibility of engine controlled parameters will fit into this envelope. The assessment of the distance of real design to this total optimum will help in deciding what change will be worthwhile for the next design improvement. Simultaneously, the holistic approach described below may take all significant vehicle and powertrain features into consideration as early as during concept stage of development.

Main Steps of New Approach to ICE Optimization

The authors used the previous experience and tools based on in-house development (knowledge database DASY [5], described below, in connection with specific codes, e.g., for mechanical loss estimation - [9], turbocharger parameters definition - [10], crankshaft safety factors assessment - [8], etc.) together with commercial software products (e.g., GT Suite).

Let's start with simple coefficient-based analysis to find the degrees of freedom for engine mass-specific power. The details are described in Appendix 1. It has used the basic relation for mean piston speed and well-known dependence between brake mean effective pressure, brake efficiency, air excess and inlet manifold or boost pressure together with inlet temperature using SAE definitions of cylinder gas exchange coefficients - [12]. Moreover, using peak pressure dependence on boost pressure and compression ratio, the approximate proportionality between peak pressure and brake mean effective pressure can be found (proportionality coefficient k_{max}). The crankshaft and all engine decisive bearings are stress- and pressure/speed limited. In the case of crank, the dependence of stress may be reflected by crank web width relative to engine bore D (web axial length coefficient K_w) and, of course, by the designed cylinder bore spacing CS. In the case of bearings, the averaged pressure and surface speed should be taken into account (p_B, c_B). Moreover, stroke-to-bore ratio ξ is important for engine mass. The engine mass m can be expressed in terms of averaged material density ρ_m and dimension/mass coefficients, which are different for engine length, height and width. That is why, the independent mass coefficients, related to the bore and linking cylinder bore spacing, cylinder bore and piston stroke (K_{CS}, K_D and K_S), were used. Then, the mass-specific brake power P_e/m can be found with respect to the number of strokes per complete cycle τ_z (namely four or two):

$$\frac{P_e}{m} = \frac{p_B c_B}{\pi K_D K_S \tau_Z \rho_m k_{max}} \cdot \frac{\left(1 - \frac{2K_W}{K_{CS}}\right)\xi}{D} \qquad (1)$$

The negative influence of large bore and too large peak pressure coefficient on engine mass is demonstrated here clearly if all other coefficients are fixed. The decisive role of coefficient ratio K_W/K_{CS} and that of stroke/bore ratio are clear from this relation, as well. The crankshaft bearing diameter is not explicitly visible from the last relation, but it can be easily found from the limit of bearing pressure if $p_B C_B$ is set. The maximum specific power influenced by K_W/K_{CS} ratio and stroke/bore ratio cannot be found before crankshaft fatigue stress is kept below the limit depending on journal and web dimensions together with stroke. That is why the simple coefficient-based analysis is not feasible for this task, even if coefficients are found from different prototype designs.
Moreover, too small cylinder bore and peak pressure coefficient may be harmful for brake efficiency because it reduces air-to-fuel ratio, limits compression ratio and thermal

efficiency of idealized thermodynamic cycle, increases cooling heat loss and makes mixture formation by direct injection more difficult.

If engine brake power and engine length x height are fixed the number of cylinders is determined - [5], i.e., bore is fixed, as well.

As a result of this analysis, the number of degrees of freedom is limited if all constraints are taken into account while downsizing the engine aiming at the best power/to/weight ratio. On the other hand, non-linear relations between free parameters may be taken into account fairly if more complex analysis is done. The links between engine thermodynamic features and vehicle powertrain design have to be respected and unprejudiced multi-criteria optimization has to be carried on.

The reference diesel engine of 1.65 dm^3 displacement with conservative dimensions (bore of 80 mm, stroke of 82 mm) and bmep of 25 bar in the range of 1 000 - 4 000 rpm was used as an initial prototype to be downsized and, if necessary, downspeeded. The initial parameters, including pressure losses, discharge coefficients and mechanical efficiency, are based on real engine tests.

Brake mean effective pressure (bmep) has been increased up to 35 bar during the current optimization, keeping the power at different speeds equal to the initial diesel engine. The displacement of all new downsized engines was thus reduced. The stroke was either unchanged, keeping mean piston speed without change (no downspeeding neither in rpm nor in mean piston speed), or it was a free parameter to be optimized in certain cases (distinguished in the explanations below from the former approach as optimized mean piston speed C_S). The latter case leads both to downspeeding or overspeeding in terms of mean piston speed. Optimization of stroke was performed for any operation point in an independent way, i.e., not taking engine optimum design for other speeds into account. The sensitivity to this practically hardly applicable measure is commented below.

No other constraints were limited during thermodynamic optimization, as, e.g., peak pressure as well as piston surface temperature, turbine inlet temperature or valve temperatures, which has created novel approach, yielding unprejudiced view on the total optimum of efficiency of the optimized engine.

Other novelty of this approach, besides very tolerant optimization constraints (if any) described in Chapter “Engine Efficiency Optimization”, is a direct coupling of thermodynamic optimum results to engine design changes, reflected by engine dimensions (dependent, e.g., on bore spacing, influenced by crankshaft dimensions fitted to peak pressures in a cylinder, as mentioned above) and to mechanical loss estimation of more detailed cranktrain model with friction described by Stribeck curves - [9]. The crankshaft was optimized using simple approximation of stress concentration factors in dependence on journal and web dimensions - [8]. The initial values were tested at the realized engine design. Accordingly, the dimensions of valves and manifolds were changed during the optimization in dependence on optimum engine dimensions, and the mass of the whole engine has been predicted. The inevitable tool for this approach has to link the data of different codes during optimizations.

The new generation of Design Assistance System DASY [8] has been employed. A scheme of data flows with future amendments up to vehicle data is presented in Figure 16 (in Appendix 3). In the current paper, the parameters up to cylinder block and cylinder head mass were predicted as a feedback to thermodynamic optimization.

Design Assistance System

To automate solution process and provide integration with CAD software, the new version of Design Assistance System - [5] - (DASY2 or DASY) has been developed. The system features descriptive model definition, numerical solvers and optimization algorithms. Any model in DASY is described with available knowledge, and definition of input and output parameters is separated from the model definition. This allows swapping of input and output parameters. It solves both direct and reverse design tasks.

Model Definition

Model in DASY2 is represented as a set of blocks linked with connections. Each block contains a set of equations, which are defining its sub-model. Sandbox approach is used for each block, which means that parameters used in equations of this block are accessible by this block only. To connect parameter of first block with parameter of second block a connection should be used. Connection provides a bridge between two separate block sandboxes. Connected parameter values are assumed to be equal. This approach allows implementation of any model with blocks, representing sub-models, and connections that will connect output state parameters of one block (sub-model) with input state parameters of another block (sub-model). With such descriptive definition one can use any knowledge about the model without strict separation of input and output parameters.

Numerical Solver

Any model implemented in DASY2 is represented with blocks and connections. This allows almost effortless structural changes. But under the cover - it is a system of non-linear algebraic equations collected from all blocks with respect to connections. Before solving this system some simplifications can be done, like merging parameters that are connected, substituting constant parameters with numbers, or performing algebraic operations on numbers. After all possible preliminary simplifications are done, numerical solver should be used to solve this system. Two numerical solvers are implemented in DASY2:

- Descend gradient solver with variable step,
- Gauss-Newton solver with variable step.

Usually, the modified Gauss-Newton solver is preferred, because it is one of the most robust gradient-based methods. This method can be seen as a modification of Newton's method for finding a minimum of a function. More details about Gauss-Newton method can be found in Appendix 4.

Integration of Simulations with CAD Systems

Integration with CAD is done using special CAD system plugins. Currently plugins to interact with CATIA and Pro/Engineer are developed. Plugin represents a communication interface between DASY and corresponding CAD system. It allows generalization of interaction with CAD and provides one convenient interface to interact with all supported CAD systems.

Using this approach, it is possible to read and write parameters from/to CAD model. It is also possible to read all available inertia properties. If some parameters or inertia properties are read from CAD model, then this model will be involved in solution process, described in previous section. If parameters are only written to CAD model - it will be updated after computation is done.

CAD model in DASY is represented as a CAD block, which can be connected to other blocks using regular connections. This ensures that CAD models are always updated with the latest parameter values and allows us to use all available data from CAD models in computation and/or optimization.

Engine Efficiency Optimization

Constraints and Basic Boundary Conditions

The thermodynamic optimization was based on calibrated 1-D model of diesel engine in GT-Power. The original 4-cylinder engine has bore/stroke 80/82 mm, as described above.

All initial dimensions and loss coefficients were taken from this real engine for both aerodynamic and mechanical losses. The combustion, represented by semi-predictive three-term ROHR Vibe function with the main phase 0-95% duration dependent on air excess and speed, was used, according to Woschni approach with modifications taking into account changes relative to reference burn duration at reference air excess and engine speed. It is decisive for cycle efficiency, other factors (e.g., Vibe shape parameters) are not significant - [13] or [14]. The reference burn duration was not fully optimized to limit the degrees of freedom but two cases of rather short and extremely short duration (35°CA or 20°CA) were used at reference A/F ratio and speed. The examples of resulting burn duration (0-90%) can be found in Figure 6.

A simplified FEM model of cooled walls was used for fire surface temperature assessment at all components in contact with gas in a cylinder. Woschni heat transfer formula was applied, up to now without correcting multipliers. Thermodynamic properties of gases, including equilibrium products of combustion, have been applied.

Turbocharger maps were created for a virtual compressor (not limited by surging or choking but using reasonable compressor efficiency dependent on compressor pressure ratio) and turbine map derived from original one by multiplier of mass flow rate which substituted the VNT, again with feasible averaged rated efficiency - [10]. They are relevant for downsized engine, in the case of significant progress in turbocharger efficiency they can be easily changed. The turbine efficiency reached at the engine takes into account the pulsations in exhaust system, i.e., blade-speed ratio and pressure ratio shifts of turbine working point. Otherwise, the turbine diameter was optimized considering the optimum usage of turbine map. This approach is very important for finding limits of ultimately achievable brake efficiency. The specific matching of a compressor and a turbine has to be done later but the limits for comparison to ideal case have been already set. Engine friction loss model in dependence on cylinder pressure pattern has been applied from [9].

Since the task was to find the best engine for each operation condition, the optimization constraints were pushed far behind the border of real engine limits, and extreme flexibility of control was assumed. The rate of heat release was optimized as well, but considering its position and duration only, since the shape is not very important in a wide range of shape changes - e.g., [1]. Two optimized variants of reference length of combustion 20 and 35 degrees CA were applied as reference cases and recalculated by Woschni combustion duration dependence on speed (duration proportional to the square root of engine speed) and air excess (duration reversely proportional to the 0.6 power of air excess).

Mixture strength (i.e., boost pressure), compression ratio up to 18 and all currently variable engine data (combustion timing, valve timing and a virtual turbocharger matching, surrogating two-stage turbocharger group) have been optimized as well, in dependence on engine speed and brake mean effective pressure at speed-appropriate constant power.

The whole turbocharging group was replaced by a virtual turbocharger with multipliers of size and speed. The turbocharger was adjusted by multipliers to required flow rate and for demanded boost pressure at any operation point. There were two optimized variants of the total two stage turbocharger group efficiency of 50% and 60% (defined from isentropic enthalpy difference at compressor and turbine sides, including compressor side intercooling and all pressure losses). The size of valves and ports and dimensions of combustion chamber in piston were proportionally modified to engine bore.

The optimized engine features fixed torque output defined by 25 bar of bmep in the whole engine speed range from 1000 to 4000 rpm. The PID controller was employed to set the injection amount to reach the required torque. Downsized versions were made by reducing engine displacement volume to keep the output parameters at the same level by increasing engine specific outputs. The engine was downsized in two steps with 30 and 35 bar of bmep using two approaches to piston stroke.

In the first one, the mean piston speed was kept constant and reduced was only engine bore. In the second one, the bore/stroke ratio was variable in a wide range.

The genetic optimization algorithm was used to search for the optimum settings of parameters listed above. The genetic algorithm was applied with 72 designs in one generation and 30 generations. The bsfc was minimized to find the highest possible value of all efficiencies.

Results of Cycle Optimization

The fuel consumption for several optimized variants at 1 000, 2 000 and 4 000 rpm is displayed in Figure 1 and Figure 3. The positive influence of higher specific load can be observed if engine speed is high enough. At lower speeds, the stagnation of bsfc at speeds lower than 2 000 rpm can be found. The significance of high turbocharger total efficiency is obvious. Additional reduction of fuel consumption can be achieved by optimization of bore/stroke ratio for given operation conditions. A little surprisingly, the peak pressure was kept limited to reasonable and achievable values, although it was unlimited during optimization - Figure 5. In addition, the advantage of very short combustion duration is not prominent, which limits the contribution of HCCI-like combustion. In all cases, reasonably short combustion (reference duration of 35°CA) is better than extremely short one. Moreover, the start of combustion is not located very early, which is visible from indicator diagrams in Figure 12.

Too low exhaust gas temperature, indicating too efficient cycle (featured by low temperature - low heat loss), creates an obstacle for reaching high boost pressure without reaching too high loss in pumping loop work. Too high air-to-fuel ratio requires very high boost pressure but yields only low exhaust gas enthalpy (temperature, compare Figure 4 - air excess and Figure 5 - turbine inlet temperature). It is followed by higher pressure upstream of a turbine, which ensures turbine power but causes significant negative pumping work.

Constant initial piston speed should be changed to optimum, which is greater at low engine speeds, as demonstrated below in Figure 6 or, in terms of stroke, in Figure 4.

These features are a result of holistic approach to engine efficiency, which takes into account the conditions for boost pressure achievement, as well. The selected results of optimized downsized engine with optimized mean piston speed, total turbocharger efficiency 60%, reference combustion duration 35 deg and bmep 30 bar are presented as examples in Figures 4, 5, 6.

Optimization does call for neither for rpm reduction nor for mean piston speed reduction, which might be slightly surprising. Even the optimum stroke is reached with higher mean piston speed than that of prototype engine. Despite very short burn duration and obvious mechanical efficiency increase (Figures 1 and 3) the bsfc at low speed is not too satisfying in comparison to medium speeds range.

The trend to long-stroke engine optimized for very low speed is changed at high speed due to the need of filling a cylinder via sufficiently large valves - Figure 6. The same trend features compression ratio, being optimized to lower values (and thus to lower temperatures at the end of compression) at low speed. These results are supported by found optimum valve timing, which prefers Miller-type cycle, while Atkinson one has only small handicap if compared to Miller.

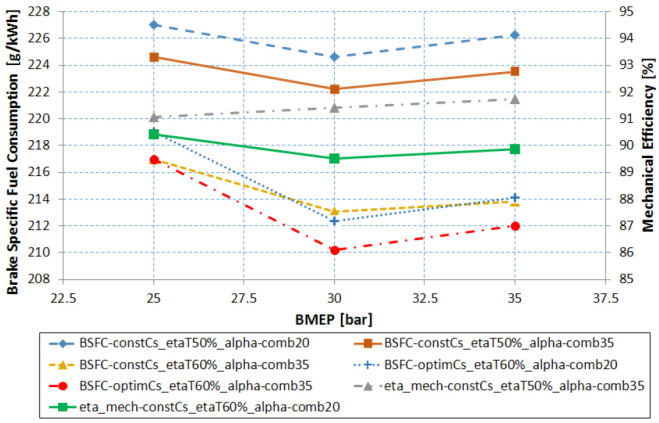

Figure 1. Optimization results - brake specific fuel consumption and mechanical efficiency as a function of engine load for engine speed 1 000 rpm and different engine optimization constraints (defined by constant or optimized mean piston speed, total turbocharger efficiency and combustion duration defined by the reference combustion angle).

While exhaust energy percentage increases with engine speed slightly (Figure 6) together with turbine inlet temperature (Figure 5) at fixed or even slightly increased bsfc, cooling loss - energy removed due to heat transfer - is reduced (Figure 6) while speed increases.

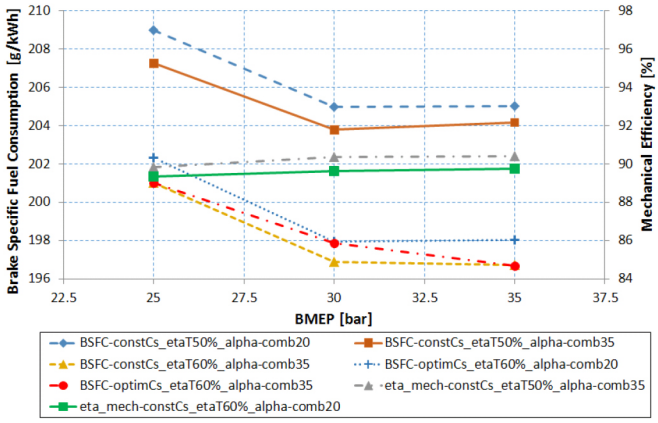

Figure 2. Optimization results - brake specific fuel consumption and mechanical efficiency as a function of engine load for engine speed 2 000 rpm and different engine optimization constraints (defined by constant or optimized mean piston speed, total turbocharger efficiency and combustion duration defined by the reference combustion angle).

This trend is supported by increased mean temperature of piston surface is a general feature for all cases of optimization and all bmep values.

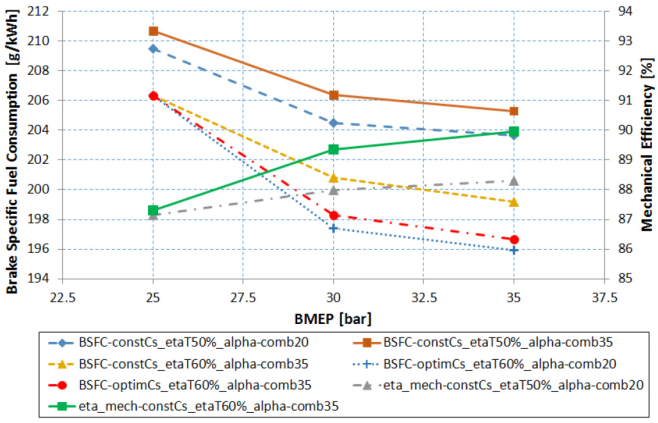

Figure 3. Optimization results - brake specific fuel consumption and mechanical efficiency as a function of engine load for engine speed 4 000 rpm and different engine optimization constraints (defined by constant or optimized mean piston speed, total turbocharger efficiency and combustion duration defined by the reference combustion angle).

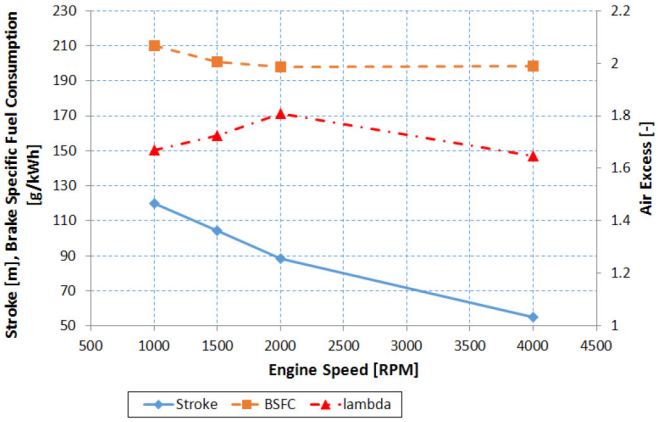

Figure 4. Optimization results - piston stroke, brake specific fuel consumption and air excess as a function of engine speed for engine with optimized mean piston speed, total turbocharger efficiency 60% and burn duration for the reference combustion angle 35 deg at bmep of 30 bar.

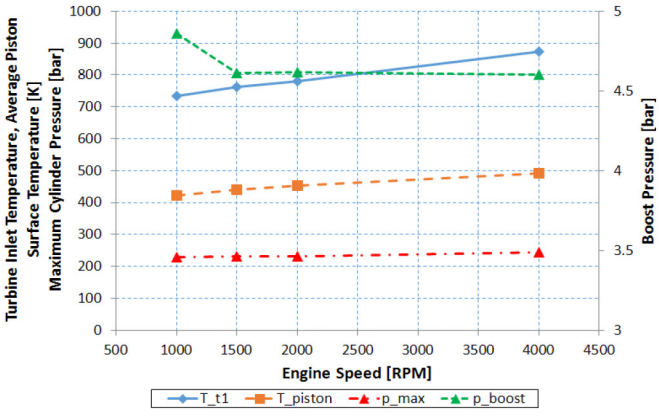

Figure 5. Optimization results - turbine inlet temperature, piston temperature, peak cylinder pressure and boost pressure as a function of engine speed for the engine with optimized mean piston speed, total turbocharger efficiency 60% and reference combustion duration (0-95%) 35 deg CA at bmep of 30 bar.

To investigate better the low-speed behavior of the engine the percentage of cooling heat loss has been investigated more carefully, see Figure 7, together with mean piston surface temperature, Figure 8. The trend is more prominent at higher bmep and does not depend on other optimized parameters for both burn durations (only better bsfc case is presented in figures). The suspicion on the main reason for it - heat transfer coefficient - is thus proven almost for sure. There is no reason to state finally that simulation of heat transfer coefficient using Woschni formula is erroneous. Nevertheless, the future investigation will be focused on sensitivity analyses (using alternative heat transfer coefficient formulae) and following experimental validation of integral heat flux from an engine in dependence on speed at high bmep, especially if downspeeded. For the optimization results, the right heat transfer speed dependence is of utmost importance. It should confirm or deny the significant increase of bsfc at downspeeded operation and the trend to optimal increased stroke at low speed together with reduction of optimal compression ratio.

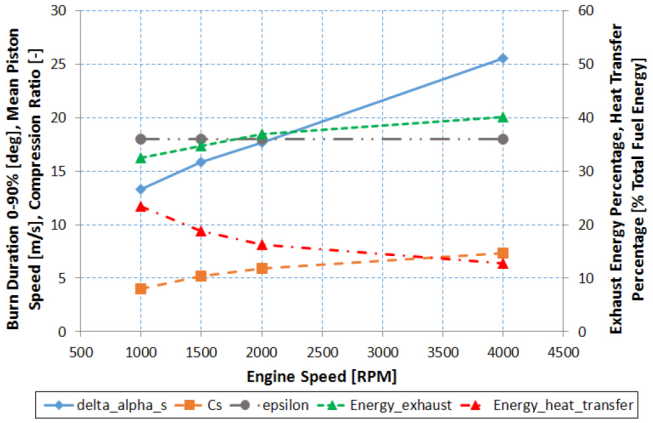

Figure 6. Optimization results - achieved burn duration 0-90%, mean piston speed, compression ratio, exhaust energy percentage and heat transfer energy percentage as a function of engine speed for the engine with optimized mean piston speed, total turbocharger efficiency 60% and reference combustion duration (0-95%) 35 deg CA at bmep of 30 bar.

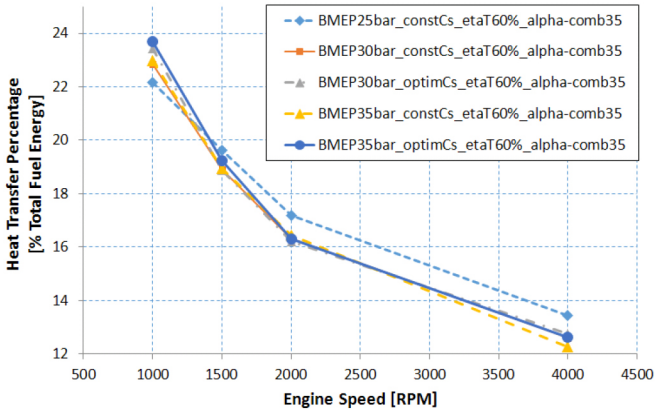

Figure 7. Cooling heat transfer percentage as a function of engine speed for the engine with different mean piston speed, total turbocharger efficiency 60% and reference combustion duration (0-95%) 35 deg CA at different bmep.

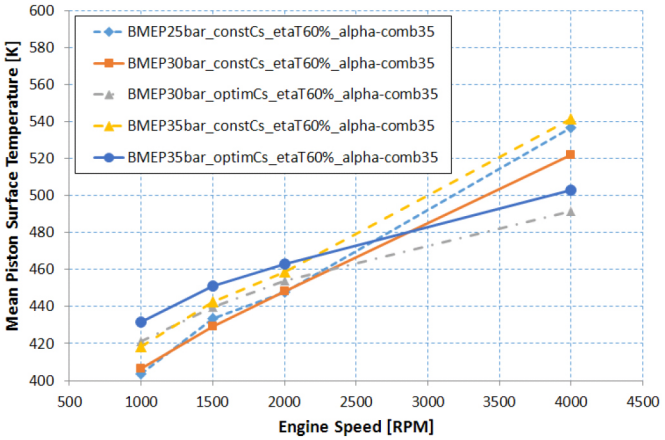

Figure 8. Mean temperature of piston surface as a function of engine speed for the engine with different mean piston speed, total turbocharger efficiency 60% and reference combustion duration (0-95%) 35 deg CA at different bmep.

The question of further reduction of bsfc cannot be solved by increased efficiency of high-pressure part of working cycle if heat transfer to walls is not reduced. The disaster with low heat rejection (uncooled) engines in mid-eighties is still remembered. The issue consists in the need for heat transfer reduction not in reduction of cooling heat flux from the engine. The insulated wall temperature should react fast to the changes of gas temperature in a cylinder not just average the mean cycle temperature. The realization of the former case is still under not very successful investigation, unfortunately. The latter case causes warming-up the gas during inlet and compression strokes (reducing charging efficiency and increasing compression work) but still keeping high heat rejection during combustion and a part of expansion and exhaust. It results in high exhaust temperature but the impact on cycle efficiency is negligible. Moreover, the porous deposit layer on the walls of a diesel engine is burnt and the natural insulation is just lost. This Woschni's hypothesis has been recently re-invented by unpublished results at a diesel engine using different blended fuels of hydrocarbons with different carbon chain length. The low-inertia and durable wall-insulation layer waits yet for new material inventions.

In the meantime, pumping loop work reduction by high-efficiency turbochargers, low-pressure loss exhaust gas aftertreatment devices and waste heat recovery (low-temperature) cycles may bring some remedy for the total brake efficiency. While the first way is illustrated clearly by the trends of bsfc in dependence on virtual turbocharger efficiency (values up to 65% might be feasible for future small two-stage turbocharger groups), high-pressure, closed-coupled aftertreatment systems may decrease the pressure losses.

Any EGR system tends on the other hand to increase bsfc in principle, if it is not used simultaneously as an additional boost control device. From that reason EGR has not been taken into account in this study.

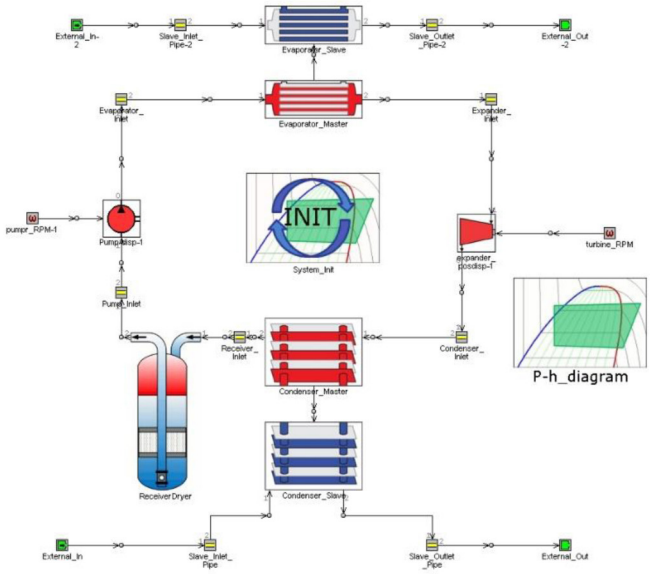

Figure 9. Scheme of an OCR system used for additional improvement of an ICE brake efficiency.

The use of waste heat may provide efficiency increase if no turbo compounding but steam or ORC is used with minimum impact on pumping loop of the engine. If thermodynamic features are taken into account, the impact is overall prospective. The results of ORC system with low-temperature boiling liquid can be simulated in GT-Cool, as presented schematically in Figure 9. The boundary conditions are created by exhaust energy percentage, temperature available at turbocharger turbine outlet and ORC efficiency depending on (evaporator) inlet and (condenser) outlet temperatures. Those boundary conditions are presented in Figure 10 and Figure 11. If the ORC total efficiency η_{ORC}, the turbine outlet temperature T_{t2} and exhaust energy percentage downstream of a turbine $E_{exh,\%}$ is taken into account, the relevant temperature difference of exhaust gas compared to enthalpy definition (zero at T_{ref}, usually 298K) has to be taken into account. Then, respecting the normalization of energy percentages $E_{exh,\%}$ to engine inlet fuel chemical energy, the contribution of ORC to engine efficiency measured in percent points is

$$\Delta\eta_e = \frac{T_{t2} - T_{ORC,in}}{T_{t2} - T_{ref}} E_{exh,\%}\eta_{ORC} \qquad (2)$$

Using mean data from Figure 10 and Figure 11 for optimized cycles and ORC efficiencies in the range of 15-25% according to the ORC simulations, the potential of ORC may be 3 - 4% percentage points. The main issue is that using extraction of heat from exhaust gas enthalpy, all heat rejected at low temperature end from ORC must be transferred to the environment via heat exchanger (unlike just throwing exhaust gas enthalpy into environment without ORC). The dimensions of low-temperature heat exchanger are very large, loading the vehicle by additional mass and volume. This issue should be assessed by the coupled CAD system in the future, as well.

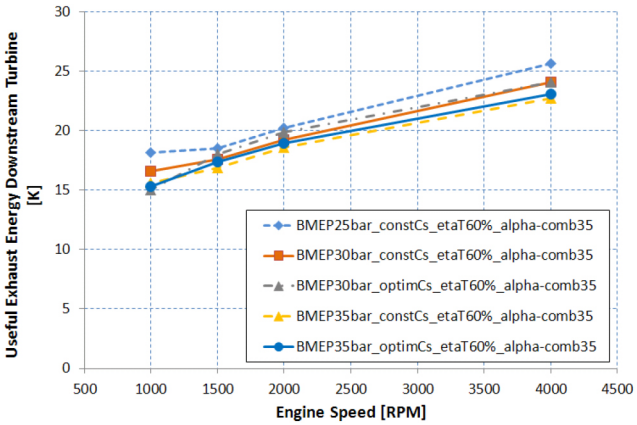

Figure 10. Exhaust energy percentage downstream of a turbine as a function of engine speed for the engine with different mean piston speed, total turbocharger efficiency 60% and reference combustion duration (0-95%) 35 deg CA at different bmep.

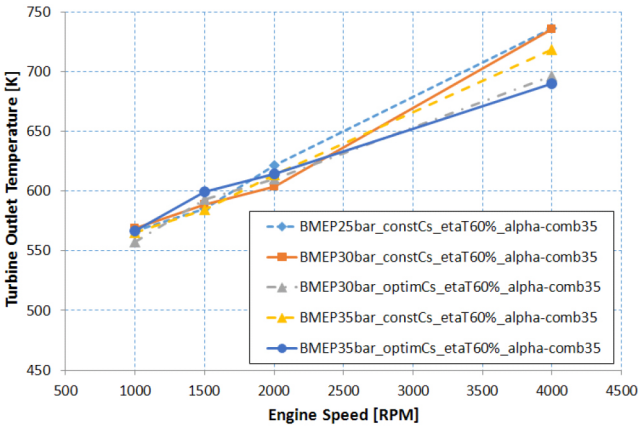

Figure 11. Temperature downstream of a turbine as a function of engine speed for the engine with different mean piston speed, total turbocharger efficiency 60% and reference combustion duration (0-95%) 35 deg CA at different bmep.

Engine Design Changes during Downsizing

Crankshaft is a decisive component for bore spacing and engine weight if peak pressure is increased. Crankshaft dimensions for diesel engine (Figure 13) were optimized to minimize crankshaft mass.

Two different engine designs for optimum cycle were selected. The examples of indicator diagrams are presented in Figure 12. Optimization goal was to have minimal mass with reasonable stress fatigue safety factors and both bearing speeds and loads. Fatigue safety factors were computed in several cross-sections, as shown in [8]. Maximal allowed mean pressures in main and connecting rod journal bearings were 50 and 80 MPa and journals circumference speeds were limited by 20 m/s. DASY used Strength Pareto Evolutionary Algorithm 2 (SPEA2) for optimization.

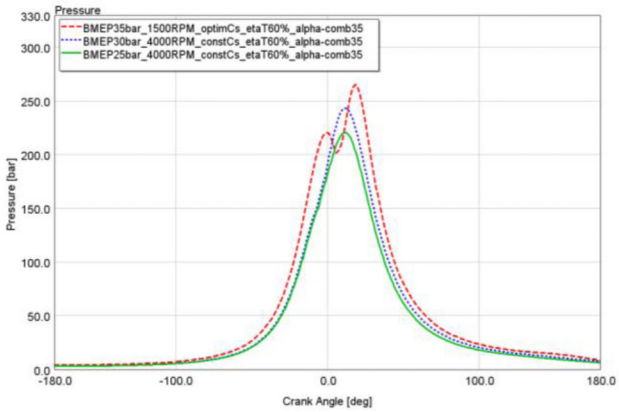

Figure 12. Cylinder pressure - crank angle diagram for crankshaft optimization (the optimum cycles - optimized stroke at different bmep and different speed).

Stress concentration factors required for fatigue safety assessment were computed using algebraic model described in [8]. In the future, it can be proven by higher level FEM analysis during the further design stage together with respecting finite stiffness of a cylinder block and main bearing supports, followed by dynamics of torsional and bending vibrations and by bearing carrying capacity checking. Nevertheless, the primary task has been to validate the feasibility of downsized engine design using preliminary design of a crankshaft and cylinder spacing.

Parameters of these designs as examples for 3 and 3.5 MPa of bmep and different strokes close to optima at 4 000 and 1 500 rpm used for optimization and optimization results are shown in Table 1 (in Appendix 2) in comparison to the original crankshaft for 2.5 MPa. The results of optimizations have shown, that with a reasonable fatigue safety factor higher than 1.5, the relative bore spacing can be kept at the same value (approx. 1.06) for a downsized engine with higher peak pressure and standard bore-to-stroke ratio. However in the case with a long stroke and high peak pressure, the results are rather different. Due to used constraints, minimal mass was obtained with a higher value of relative bore spacing and rather long connecting rod journals. The optimizer preferred to keep some journal overlap (stress concentration factors are low for it) and the bearing carrying capacity required to extend the cylinder spacing for smaller journals. Changing constraints for journal lengths different design can be obtained, as visible in the last columns of Table 1. It has bigger mass due to large journal diameter, shorter journals but thicker webs and more conventional journals lengths and diameters. The cylinder spacing is quite large, nevertheless.

Performed optimization is a preliminary study. It does not take into account all details and constraints. However, it shows the possibility to connect optimization of thermodynamics with design optimization using DASY software. Moreover, the long-stroke case has demonstrated surprising results for this highly non-linear task - Table 1. The extreme crankshaft designs are currently under deeper investigation aimed at final explanation and formulation of hints for new engine design. The result of optimization is a single solution with minimal mass and all parameters satisfying all constraints.

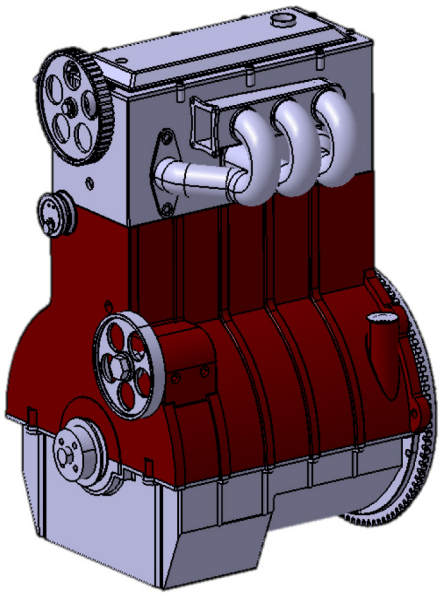

Figure 13. Engine model used for optimization.

Current optimization goal was to obtain a minimal mass of crankshaft only. The mass of crankshaft may be calculated from a parametric model in CATIA, in which change of all details (mass-reducing bores, counterweights, lateral web shapes, etc.), are scaled independently using parametric design tools. The same is valid for cranktrain components (connecting rod and piston with a piston pin). The parametric design yields the important mass details used in cranktrain force evaluation, preliminary check of crankshaft strength and bearing loads and mechanical efficiency of a downsized engine. From this point of view, Table 1 presents potential of downsized engine weight but it shows how extreme peak pressures will increase cylinder bore spacing with impacts on crankshaft (and engine) mass, as well.

Minimal mass of engine is desired in real life, however. The masses of a cylinder block and a head have to be evaluated simultaneously with optimization, as well. The independent changes of different dimensions (bore spacing, height and width of a cylinder block or a cylinder head - see also coefficients related to bore in the Equations (5) or (7)) pose some issues for very complicated shapes of those parts. From that reason, the simplified parametric CAD model was developed - Figure 14.

The main parts of a block (or a head) were split into two groups with wall thickness dependent on loads (typically cylinder wall thickness, main bearing supporting wall thickness, the walls or plates anchoring cylinder head or main bearing bolts, etc.) and load independent (all walls and covering decks sealing water or oil spaces, etc.). The wall thickness of a latter group is determined by manufacturing technology with the addition of mean thickness, calculated as mass equivalent of noise-avoiding ribs. Those thicknesses were applied separately (e.g., the bottom part of a crankcase) or just added to the thickness of loaded parts (e.g., the cylinder wall thickness). The representative thickness of unloaded walls may be found from existing design, including mass of ribs and cooling water, if necessary.

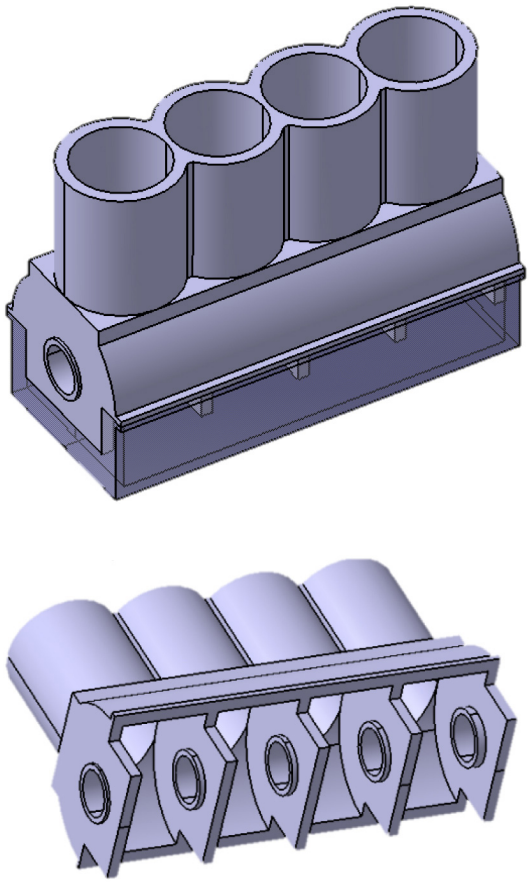

Figure 14. Simplified engine block model.

A similar approach may be used for a cylinder head. This approximation enables a designer to do parametric changes of the whole engine without solving complicated interference problems. This approach is prepared for the use in future optimizations.

Design Assistance System 2 is still under active development, but already implemented features allow its usage in real tasks. The main features are descriptive model definition, algebraic equations parser, numerical solvers, optimization algorithms, CAD and other plugins. These features allow easy model definition. Modular structure of DASY model provides a convenient way for nearly effortless structural changes and what-if studies. Definition of input and output parameters is separated from the model definition, which means that both direct and reverse design tasks can be solved. Models in DASY are organized in a way that allows easy re-usage of model parts and knowledge in different projects. Performed crankshaft optimization shows possibility to use DASY software to connect optimizations in different fields and use them in final design. The CAD parameterization can be done using simplified parametric models based on experience with previous fully designed engines.

The main reason for finding all impacts of downsizing to engine mass and dimensions concern in the assessment of vehicle duty cycle fuel consumption and emissions. Combining the achieved results for selected engine design (e.g., with fixed stroke and compression ratio), as demonstrated in Figure 15, with other vehicle parameters found in DASY, the whole

optimization according to Figure 16 may be followed with usable results even in the early stage of development. Although the wide-open throttle curve are not very good, the low load-low speed quadrant of the map offers very significant part-load fuel consumption reduction. The details will be published soon.

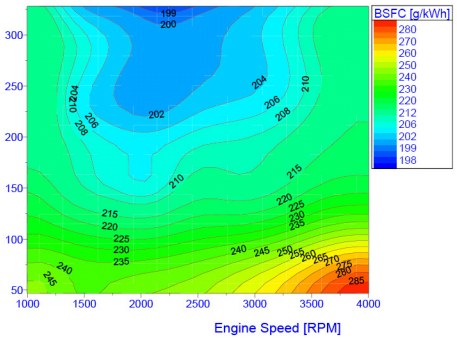

Figure 15. Optimization results - map of brake specific fuel consumption as a function of engine speed and torque for engine with displacement 1.2 liter (maximal bmep 30 bar) and stroke of 115 mm, total rated turbocharger efficiency 60% and reference combustion duration 35 deg CA.

Summary/Conclusions

Design Assistance System 2, although still under active development, has been used for a four-stroke diesel downsizing study.

The unconstrained thermodynamic optimization (no limits for peak pressure, fire surface or exhaust gas temperatures, very short duration of combustion, reasonably matched turbocharger efficiency, etc.) does not call either for extreme peak pressures or very short combustion durations. Surprisingly, new combustion patterns pertinent to HCCI-like and dual-fuel systems (PCCI, RCCI, …) may be important if connected to simpler and less expensive exhaust gas aftertreatment systems, but they do not contribute directly to engine efficiency, if the complete engine cycle (including pumping loop) is taken into account. Moreover, high level of EGR called for by those systems, cannot improve thermodynamic parameters over the limits found by the current study. The optimum angle duration of combustion is close to 30 deg CA (0-95%) for high speed, being shortened to approximately 20 deg CA at low speed. The position of combustion start is not far from top dead center. The optimum air excess values reflect in-cylinder temperatures and speed. The optimum air excess decreases with increased engine speed, allowing for lower pumping losses. Their optimum values are suitable for advanced pollutant aftertreatment systems.

The results of unlimited optimization constraints have shown the importance of cooling loss at reduced engine speed and the need of a long-stroke engine design, if low speed is used dominantly in engine operation. Optimum valve timing requires a moderate Miller cycle, compression ratio being kept at standard values of 16-18, except for reduction at lowest speeds. It is caused again by the increase of cooling loss at low speed.

Downsizing may be accompanied by downspeeding, reflected in lower cycle frequency (speed in rpm), which positively increases time for unsteady events during combustion and gas exchange while the cycle cooling loss and the threat of knocking is increased, as well, and mechanical losses are reduced. According to the current results, more can be achieved if downspeeding in terms of mean piston speed is done only by moderate mean piston speed reduction. Especially in the diesel (CI) engine case the stroke can be increased for a downsized engine, reducing mean piston speed less than proportionally to dimensions at the same engine speed while downsizing the engine. All those conclusions are closely connected with correct prediction of heat transfer to cooled walls, especially at low engine speed. The cooling loss importance should be focused by the future investigations, starting with checking validity of used empirical formulae for engine heat transfer coefficient and assessing low The efficiency limits presented in this paper for downsized small car four-stroke diesel (achieved values of 40 - 44%, optimum at 2 000 rpm) cannot be used as absolute ones. There are still some possibilities of bsfc reduction if mechanical efficiency is increased by approx. 3% or pressure losses in EGR systems are reduced. Nevertheless, those limits show that there is a problem to achieve more than 46% in any case without waste-heat recovery or extremely efficient turbochargers.

Altogether, there is only limited potential of further decreasing the total optimum of bsfc in comparison to recent achievements, namely by increasing turbocharger efficiency (accompanied by the reduction of pressure losses in pipe systems), keeping minimum necessary air excess (an advantage of RCCI, if sufficiently robust system is realized) and - if suitable method is found - reducing heat transfer to walls. The latter issue limits downspeeding, calling for rightspeeding instead.

Nevertheless, the operation at partial loads and speeds promises additional fuel savings.

The real limits of engine mass reduction were found by coupling of stress simulation to CAD parametric design. The increase of relative bore spacing by at least 15% should be expected if optimum cycle at bmep of 35 bar is applied. These results will be published soon. They are important for the holistic assessment of the rightsized engine potential in operation fuel consumption.

The next steps for diesel engines should consider compromised but fixed stroke and compression ratio of engines, especially for downspeeded designs. The comparison with envelope of achievable efficiencies and dimensions will demonstrate the yet unused potential of fully flexible engine. The further works are being already focused on assessment of low speed/load operation of engines and their dynamic response, including smart control systems and combined turbo-supercharging. Both of these features are unavoidable for vehicle road test application. The results of dynamic response simulations may employ even 3-D models, as demonstrated, e.g., in [11].

Considering future ICE improvement, the relevance of correctly simulated model of wall heat transfer inside a cylinder calls for further experimental investigation of this issue together with assessment of wall insulation by low thermal inertia materials. The second decisive factor is turbocharger or supercharger efficiency improvement. The future research will be focused on coupling waste-heat recovery cycles to current ICE performance considering the size and weight of appropriate systems with impacts to vehicle performance, which is possible in DASY.

Using DASY focused on the complete vehicle, the whole optimization according to Figure 16 may be followed with usable results even in the early stage of development. This goal is currently intensively elaborated. Other activities are being focused on the same investigation of spark ignition ICE, limited moreover by knocking, RCCI engines and to a two-stroke potential assessment. The overall goal - finding the best solution for future cars with reasonable range and environment friendly features - calls for this holistic approach used, as well, for future battery vehicles.

References

1. Eilts, P., Stoeber-Schmidt, C., and Wolf, R., “Investigation of Extreme Mean Effective and Maximum Cylinder Pressures in a Passenger Car Diesel Engine,” SAE Technical Paper 2013-01-1622, 2013, doi:10.4271/2013-01-1622.
2. Hyvonen J.: Higher Efficiency for Further Downsizing; Example from Large Bore Medium Speed Engines (Wärtsilä). High Efficiency IC Engine Symposium, SAE 2013
3. Curtis E.: Near Term Combustion System Development and the Influence of Transmissions, Drive Cycles and Fuels (Ford Motor Company). High Efficiency IC Engine Symposium, SAE 2013
4. Reitz R.: Reactivity Controlled Compression Ignition (RCCI) for Ultra-High Efficiency IC Engine Operation with Low NOx and PM Emissions Plus Transient Control. High Efficiency IC Engine Symposium, SAE 2013
5. Bogomolov, S., Mikulec, A., and Macek, J., “Development of Design Assistance System and Its Application for Engine Concept Modeling,” SAE Technical Paper 2011-37-0030, 2011, doi:10.4271/2011-37-0030.
6. Hejlsberg A., Torgersen M., Wiltamuth S., Golde P. (2010). C# Programming Language, The (4th Edition)
7. Kim Mifa, Hiroyasu Tomoyuki, Miki Mitsunori, Watanabe Shinya (2004). SPEA2+: Improving the Performance of the Strength Pareto Evolutionary Algorithm 2, *Parallel Problem Solving from Nature - PPSN VIII, 8th International Conference*, proceedings pp 742-751.
8. Bogomolov S., Mikulec A., Macek J., Valasek M., Doleček V. (2012). Knowledge-Based Design and Optimization of Engines, *THIESEL 2012 Conference on Thermo- and Fluid Dynamic Processes in Direct Injection Engines*.
9. Macek, J., Fuente, D., and Emrich, M., “A Simple Physical Model of ICE Mechanical Losses,” SAE Technical Paper 2011-01-0610, 2011, doi:10.4271/2011-01-0610.
10. Vítek, O., Macek, J., and Polášek, M., “New Approach to Turbocharger Optimization using 1-D Simulation Tools,” SAE Technical Paper 2006-01-0438, 2006, doi:10.4271/2006-01-0438.
11. Macek, J., Dolecek, V., Srinivasan, S., Tanner, F. et al., “Optimization of Engine Control Strategies During Transient Processes Combining 1-D and 3-D Approaches,” SAE Technical Paper 2010-01-0783, 2010, doi:10.4271/2010-01-0783.
12. Heywood J.B.: Internal Combustion Engine Fundamentals. McGraw Hill 1998
13. Macek J.: Optimization of Using Fuel Chemical Energy in Reciprocating Engines. Doctor of Science Dissertation, Czech Technical University 1989, 631 pp.
14. Macek J., Foglar P., Holmberg S.: The Development of Working Cycle and Design of a Four-Stroke, Medium Speed, Heavy Fuel Engine of 275 mm Bore. CIMAC Paper, Oslo 1985

Contact Information

Sergii Bogomolov
sergii.bogomolov@fs.cvut.cz

Vit Dolecek
v.dolecek@fs.cvut.cz

Jan Macek
jan.macek@fs.cvut.cz

Antonin Mikulec
antonin.mikulec@fs.cvut.cz

Oldrich Vitek
oldrich.vitek@fs.cvut.cz

Acknowledgments

This work was supported by:

- Technological Agency, Czech Republic, programme Centre of Competence, project #TE01020020 Josef Božek Competence Centre for Automotive Industry.
- EU Regional Development Fund in OP R&D for Innovations (OP VaVpI) and Ministry of Education, Czech Republic, project #CZ.1.05/2.1.00/03.0125 Acquisition of Technology for Vehicle Center of Sustainable Mobility.
- The Grant Agency of the Czech Technical University in Prague, grant No. SGS13/184/OHK2/3T/12.

This support is gratefully acknowledged.

Definitions/Abbreviations

B - bearing

bmep - brake mean effective pressure

bsfc - brake specific fuel consumption

CA - crank angle

CI - compression ignition

CR - compression ratio

CS - cylinder bore spacing

c s, cs - mean piston speed

D - diameter, cylinder bore

DASY - design assistance system

delta alpha s - combustion duration (0-95% fuel burnt) in CA

eta mech - mechanical efficiency of an engine

eta T - total turbocharger efficiency (virtual turbocharger surrogates the real two-stage turbocharging)

FEM - finite element method

FIE - fuel injection equipment

FMEP - friction mean effective pressure

GHG - green-house effect causing gases

HCCI - homogeneous charge compression ignition

H_u - lower calorific value of fuel

h - width

ICE - internal combustion engine

i_c - number of cylinders

K - dimension coefficient related to cylinder bore

k - coefficient

L - length

L_t - stoichiometric A/F ratio

lambda - air excess (relative air-to-fuel ratio)

MB - main bearing

MBL - main bearing journal length

NOx - sum of polluting nitrogen oxides

NVH - noise, vibration and harshness

n - engine speed (rpm)

ORC - Organic Rankine cycle

p boost - boost pressure in an inlet manifold

PCCI - premixed charge compression ignition

PID - proportional-derivative-integrating controller

P_e - brake power

p_e - brake mean effective pressure

p_{im} - boost pressure

p_{max}, **p max** - cylinder peak pressure

PM - particulate matter (exhaust pollutant)

RB - connecting rod bearing

RBL - connecting rod bearing journal length

RCCI - reaction controlled compression ignition

ROHR - rate of heat release

r_{im} - specific gas constant for inlet manifold contents

S - stroke

SCR - selective catalytic reduction of NOx

T_{im} - inlet manifold temperature

T piston - mean temperature of piston fire surface

T t1 - turbine inlet temperature of exhaust gas

VNT - variable nozzle turbine

V_z - engine displacement volume

W - crank web

z - ratio of fuel injected before compression to total amount of fuel

$\eta_{sc,red}$ - scavenging efficiency, reduced to oxygen contents in rest gas and/or to that of exhaust recirculated gas

η_e - brake efficiency

λ - air excess (relative air-to-fuel ratio)

λ_{ch} - charging ratio

ξ - stroke/bore ratio

τ_z - number of strokes per a single cycle

Appendix

Appendix 1

Basic relation for mean piston speed c_s and well-known dependence between brake mean effective pressure p_e, brake efficiency η_e, air excess λ and inlet manifold or boost pressure p_{im} together with inlet temperature T_{im} using SAE definitions of cylinder gas exchange coefficients - [12] yields

$$C_s = \frac{Sn}{30} = \frac{\xi Dn}{30}$$

$$p_{im} = \frac{r_{im}}{H_u}\frac{p_e}{\eta_e T_{im}}\frac{z + \lambda L_t}{\lambda_{ch}\eta_{sc,red}} \tag{3}$$

z being ratio of fuel injected before compression stroke to the total amount of fuel (typically z =0 for diesels), λ_{ch} charging ratio and $\eta_{sc,red}$ scavenging efficiency, reduced to oxygen contents in rest gas and/or to that of exhaust recirculated gas. The peak pressure may be estimated from the pressure after ideal compression, corrected by coefficient k_b

$$p_{max} = p_{im}\varepsilon^k k_b = k_b \frac{r_{im}}{H_{u}r_{im}}\frac{\varepsilon^k(z + \lambda L_t)}{\eta_e \lambda_{ch}\eta_{sc,red}} p_e, \qquad i.e.,$$

$$p_{max} = k_{max} p_e \tag{4}$$

Mean piston speed (in fact, square of it) determines acceleration of reciprocating motion and thus the inertia forces, bmep being closely connected to the peak pressure if a certain cycle type (e.g., RCCI) is assumed.

Inlet manifold temperature limit for intercooled charging is almost constant (depending, of course, on the system of charging/intercooling and on the inlet manifold or boost pressure). The cycle parameters (compression ratio ε, maximum/end-of-compression pressure ratio coefficients k, brake efficiency η_e and relative A/F ratio λ and gas exchange parameters - mixture creation key z, which is 0 or 1 according to mixture creation location and timing, charging ratio λ_{ch} and scavenging efficiency $\eta_{sc,red}$, reduced to real oxygen content in fresh charge considering EGR, are all almost fixed for the certain type of cycle used, as well.

Engine brake power depends on

$$P_e = \frac{V_z p_e n}{30\tau_z} = \frac{i_c \frac{\pi \xi D^3}{4} p_e n}{30\tau_z} = \frac{\pi \xi}{4\tau_z} i_c D^2 p_e c_s \tag{5}$$

Displacement-volume-specific brake power is

$$\frac{p_e}{V_z} = \frac{p_e n}{30\tau_z} = \frac{1}{\tau_z}\frac{p_e c_s}{D} \tag{6}$$

i.e., the smaller cylinder bore the better specific power is achieved if bmep and piston speed are limited. The same specific power is often referred to as engine mass specific, as well. Nevertheless, engine mass does not depend on all engine dimensions in the same way, i.e., the displacement volume is not enough to characterize engine mass with mean material density ρ_m. That is why, the independent mass coefficients related to the bore and linking cylinder bore spacing, cylinder bore and piston stroke (K_{CS}, K_D and K_S), were used (in other words, the dependence of engine mass on engine length, width and height - for vertical in-line cylinders - has been taken into account):

$$m = K_{CS} i_c D K_S \xi D K_D D = K_D K_S K_{CS} i_c \xi D^3 \rho_m \tag{7}$$

$$\frac{P_e}{m} = \frac{\pi}{4}\frac{1}{K_D K_S K_{CS}}\frac{p_e c_s}{\tau_z \rho_m D} \tag{8}$$

Cylinder spacing, which is decisive for engine length, can be added from individual contributions of main bearing length, connecting rod bearing length and the width of crank webs roughly, if an example of in-line engine is used. Recalculating all dimensions to length coefficients related to cylinder bore (*MBL* - main bearing length, *RBL* - connecting rod bearing length, *W* - web axial length), it yields

$$K_{CS} = K_{MBL} + K_{RBL} + 2K_W \tag{9}$$

Engine load is limited by maximum reference pressure in bearings, dependent on fatigue limit of slide bearing surface material. The reference bearing pressure can be calculated from peak pressure piston force and appropriate dimensions (diameter and length) of a bearing journal, e.g., for connecting rod bearing

$$p_{RB} = \frac{\frac{\pi}{4} D^2 p_{max}}{K_{RBD} K_{RBL} D^2} = \frac{\pi}{4} \frac{k_{max}}{K_{RBD} K_{RBL}} p_e < LIM \tag{10}$$

Additionally, the coefficient $\boldsymbol{K_{RBD}}$ linking bearing diameter and bore was introduced. The bearing pressure can be reduced increasing length and diameter of a bearing journal. Nevertheless, the bearing dissipated power caused by load x speed has to be limited simultaneously, since the lubricating oil flow rate cannot be increased freely due to length and clearance in the bearing, i.e.,

$$p_{RB} c_{RB} = \frac{\frac{\pi}{4} D^2 p_{max}}{K_{RBD} K_{RBL} D^2} \frac{\pi K_{RBD} D n}{60} = \frac{\pi p_{max}}{4 K_{RBL}} \frac{\pi S n}{60 \xi} = \frac{\pi^2 k_{max} p_e c_s}{8 K_{RBL} \xi} < LIM \tag{11}$$

This limiting factor depends on bearing length factor only, i.e., on cylinder spacing, which influences the engine length. Assuming for the sake of simplicity the same limits and lengths for main and connecting-rod bearings

$$p_B c_B = \frac{\pi^2 k_{max} p_e c_s}{4 (K_{CS} - 2K_W) \xi}, i.e.,$$

$$p_e c_s = \frac{4 (K_{cs} - 2K_W) \xi}{\pi^2 k_{max}} p_B c_B \tag{12}$$

i.e., longer stroke and narrower webs are of advantage for achievable $p_e c_s$ if $p_B c_B$ is limited. K_W and ξ are not independent on each other, however, due to crankshaft fatigue strength limit and K_{BD} has to be taken into account calculating this limit (see below).

Then, the mass-specific engine brake power is

$$\frac{P_e}{m} = \frac{p_B c_B}{\pi K_D K_S \tau_Z \rho_m k_{max}} \cdot \frac{\left(1 - \frac{2K_W}{K_{CS}}\right) \xi}{D} \tag{13}$$

Appendix 2

Table 1. Design parameters used in optimization and optimization results.

		Design #1		Design #2		Design #3		Design #3	
Parameter	**Units**	**Limits**	**Value**	**Limits**	**Value**	**Limits**	**Value**	**Limits**	**Value**
bmep	MPa	fixed	2.5	fixed	3	fixed	3.5	fixed	3.5
max. pressure in cylinder	MPa	fixed	21.89	fixed	24.16	fixed	27.45	fixed	27.45
bore	mm	fixed	80	fixed	73.03	fixed	61.23	fixed	61.23
stroke	mm	fixed	82	fixed	82	fixed	100	fixed	100
engine speed	1/min	fixed	4000	fixed	4000	fixed	4000	fixed	4000
bore spacing	mm	[85; 130]	85	[78; 130]	78	[65; 120]	82.19	[65; 120]	85.63
relative bore spacing	-	-	1.06	-	1.07	-	1.34	-	1.4
mass	kg	-	14.99	-	12.78	-	11.4	-	13.35
minimal safety factor	-	≥ 1.5	1.5	≥ 1.5	1.5	≥ 1.5	1.5	≥ 1.5	1.5
conrod journal length	mm	[10; 40]	25	[10; 40]	24.53	[10; 40]	30.3	[10; 24]	21.52
main journal length	mm	[10; 40]	25.18	[10; 40]	23.1	[10; 40]	17.62	[10; 24]	17.97
conrod journal diameter	mm	-	55.05	-	51.53	-	33.33	-	46.94
main journal diameter	mm	-	87.4	-	87.63	-	91.7	-	89.95
web thickness	mm	≥ 10	13.41	≥ 10	11.18	≥ 10	11.09	≥ 10	12.63
conrod radius	mm	fixed	2	fixed	2	fixed	2	fixed	2
main radius	mm	fixed	2	fixed	2	fixed	2	fixed	2
conrod bearing speed	m/s	≤ 20	11.53	≤ 20	10.79	≤ 20	6.98	≤ 20	9.83
main bearing speed	m/s	≤ 20	18.3	≤ 20	18.35	≤ 20	19.2	≤ 20	18.84

Appendix 3

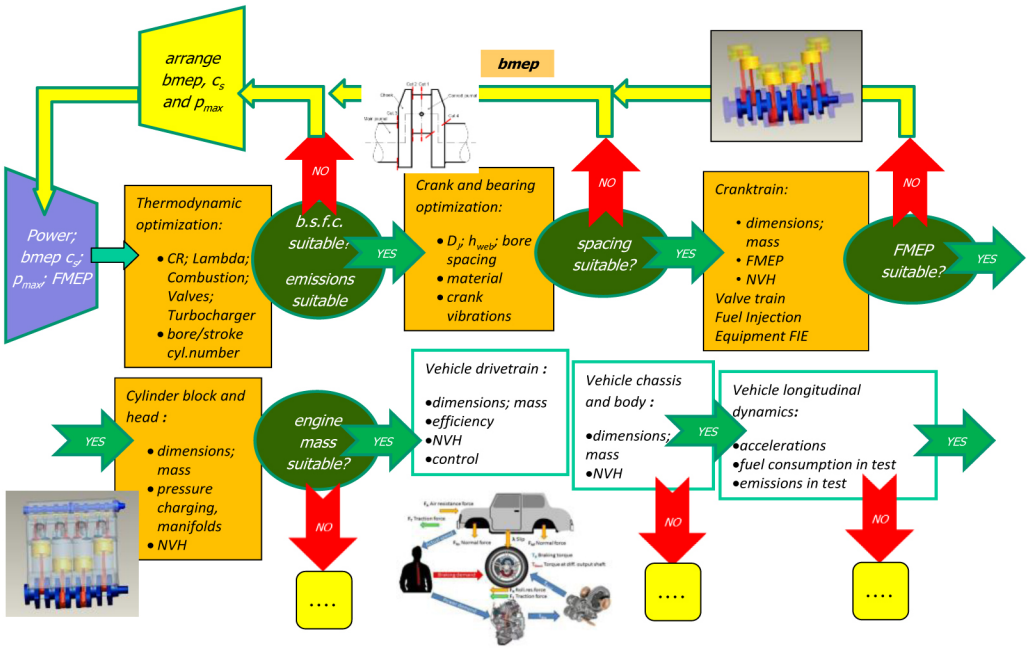

Figure 16. Data flows during coupled thermodynamic and design optimization.

Appendix 4

Gauss-Newton method

The idea of Newton's method is as follows: one starts with an initial guess which is reasonably close to the true root, then the function is approximated by its tangent line, and one computes the x-intercept of this tangent line (which is easily done with elementary algebra). This x-intercept will typically be a better approximation to the function's root than the original guess, and the method can be iterated. Iteration of this method is as follows:

$$x_{n+1} = x_n - \frac{f(x_n)}{f'(x_n)}, \qquad n \geq 0$$

(14)

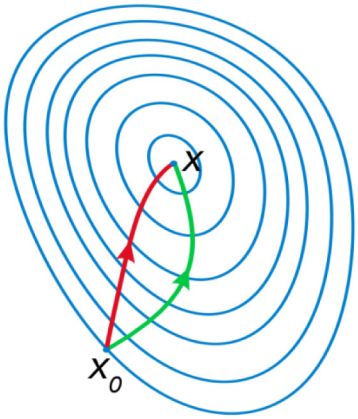

Figure 17. Newton's method in optimization.

Newton's method in optimization is specialized to find stationary points of differentiable functions, which are the zeroes of the derivative function (Figure 17). Newton's method attempts to construct a sequence x_n from an initial guess x_0 that converges towards x_* such that $f'(x_*) = 0$. This x_* is called a stationary point of $f(x)$. The second order Tylor expansion $f_T(x)$ of function $f(x)$ around x_n (where $\Delta x = x - x_n$) is:

$$f_T(x_n + \Delta x) = f_T(x) = f(x_n) + f'(x_n)\Delta x + \frac{1}{2}f''(x_n)\Delta x^2$$

(15)

and attains its extreme when its derivative with respect to Δx is equal to zero, i.e. when Δx solves the linear equation:

$$f'(x_n) + f''(x_n)\Delta x = 0$$

(16)

Thus, provided that $f(x)$ is twice-differentiable function well approximated by its second order Tylor expansion and the initial guess x_0 is chosen close enough to x_*, the sequence (x_n) defined by:

$$\Delta x = x - x_n = -\frac{f'(x_n)}{f''(x_n)}$$

(17)

$$x_{n+1} = x_n - \frac{f'(x_n)}{f''(x_n)}, \qquad n \geq 0$$

(18)

will converge towards a root of f', i.e. x_* for which $f'(x_*) = 0$.

The above iterative scheme can be generalized to several dimensions by replacing the derivative with the gradient, $\nabla f(x)$, and the reciprocal of the second derivative with the inverse of the Hessian matrix, $Hf(x)$. One obtains the iterative scheme

$$x_{n+1} = x_n - [Hf(x_n)]^{-1}\nabla f(x_n), \qquad n \geq 0$$

(19)

Usually Newton's method is modified to include a small step size $\gamma > 0$ instead if $\gamma = 1$

$$x_{n+1} = x_n - \gamma[Hf(x_n)]^{-1}\nabla f(x_n), \qquad n \geq 0$$

(20)

The Gauss-Newton algorithm is a method used to solve non-linear least squares problems. Unlike Newton's method, the Gauss-Newton algorithm can only be used to minimize a sum of squared function values, but it has the advantage that second derivatives, which can be challenging to compute, are not required. Given m functions $r = (r_1,\ldots,r_m)$ of n variables $\beta = (\beta_1,\ldots, \beta_n)$, with $m \geq n$, the Gauss-Newton algorithm iteratively finds the minimum of the sum of squares

$$S(\beta) = \sum_{i=1}^{m} r_i^2(\beta)$$

(21)

Starting with an initial guess $\beta^{(0)}$ for the minimum, the method proceeds by iterations

$$\beta^{(s+1)} = \beta^{(s)} - (J_r^T J_r)^{-1} J_r^T r\left(\beta^{(s)}\right),$$

(22)

where

$$J_r = \frac{\partial r_i}{\partial \beta_j}\left(\beta^{(s)}\right)$$

(23)

is the Jacobian matrix of r and the symbol T denotes the matrix transpose, and $(J_r^T J_r)^{-1} J_r^T$ is left-inverse of Jacobian matrix. The assumption $m \geq n$ in the algorithm statement is necessary, as otherwise the matrix $J_r^T J_r$ is not invertible and the normal equations cannot be solved (at least uniquely). Iterations relation can be rewritten as

$$\beta^{(s+1)} = \beta^{(s)} + \Delta,$$

(24)

where

$$\Delta = -(J_r^T J_r)^{-1} J_r^T r\left(\beta^{(s)}\right)$$

(25)

With the Gauss-Newton method the sum of squares S may not decrease at every iteration. However, since Δ is a descent direction, unless $S(\beta^{(s)})$ is a stationary point, it holds that $S(\beta^{(s)} + \alpha\Delta) < S(\beta^{(s)})$ for all sufficiently small $\alpha > 0$. Thus, if divergence occurs, one solution is to employ a fraction, α, of the increment vector, Δ, in the updating formula

$$\beta^{(s+1)} = \beta^{(s)} + \alpha\Delta$$

(26)

In other words, the increment vector is too long, but it points in “downhill”, so going just a part of the way will decrease the objective function S. An optimal value for α can be found by using a line search algorithm, that is, the magnitude of α is determined by finding the value that minimizes S, using some search method in the interval $0 < \alpha < 1$.

Gauss-Jordan elimination (also known as row reduction) is used to compute an inverse of square matrix ($J_r^T J_r$). To perform row reduction on a matrix, one uses a sequence of elementary row operations to modify the matrix until the lower left-hand corner of the matrix is filled with zeros, as much as is possible. There are three types of elementary row operations:

- swapping two rows,
- multiplying a row by a non-zero number,
- adding a multiple of one row to another row.

Using these operations, a matrix can always be transformed into an upper triangular matrix, and in fact one that is in row echelon form. Once all of the leading coefficients (the left-most non-zero entry in each row) are 1, and in every column containing a leading coefficient has zeroes elsewhere, the matrix is said to be in reduced row echelon form. This final form is unique; in other words, it is independent of the sequence of row operations used.

The Engineering Meetings Board has approved this paper for publication. It has successfully completed SAE's peer review process under the supervision of the session organizer. The process requires a minimum of three (3) reviews by industry experts.

ISSN 0148-7191

http://papers.sae.org/2014-01-1098